Nuclear Materials and Energy 3–4 (2015) 1–5

Contents lists available at ScienceDirect

Nuclear Materials and Energy

journal homepage: www.elsevier.com/locate/nme

Electrical behaviour of ceramic breeder blankets in pebble form after γ-radiation

E. Carella[a,b,*], T. Hernández[a], B. Moreno[c], E. Chinarro[c]

[a] National Fusion Laboratory — CIEMAT, Avda. Complutense 40, 28040 Madrid, Spain
[b] UNED Foundation, C/ Francisco de Rojas, 2, 28010 Madrid, Spain
[c] Instituto de Cerámica y Vidrio (CSIC), C/Kelsen 5 28049 Madrid, Spain

ARTICLE INFO

Article history:
Received 14 October 2014
Revised 11 February 2015
Accepted 12 February 2015
Available online 16 May 2015

Keywords:
Irradiation effect
Electrical conductivity
Ionizing radiation
Solid breeder blanket

ABSTRACT

Lithium orthosilicate (Li_4SiO_4) ceramics in from of pebble bed is the European candidate for ITER testing HCPB (Helium Cooled Pebble Bed) breeding modules. The breeder function and the shielding role of this material, represent the areas upon which attention is focused. Electrical measurements are proposed for monitoring the modification created by ionizing radiation and at the same time provide information on lithium movement in this ceramic structure. The electrical tests are performed on pebbles fabricated by Spray-dryer method before and after gamma-irradiation through a ^{60}Co source to a fluence of 4.8 Gy/s till a total dose of $5 * 10^5$ Gy. The introduction of thermal annealing treatments during the electrical impedance spectroscopy (EIS) measurements points out the recombination effect of the temperature on the γ-induced defects.

1. Introduction

The breeder blanket system (BBs) is one of the key components for future fusion reactor due to its multiple functions as tritium breeder, neutron/gamma-ray shielding, and convertor of the kinetic energy of fusion neutron and secondary gamma rays into heat. It is based on lithium, which can generate tritium by the ^6Li (n, α) T or ^7Li $(n, n\alpha)$ T nuclear reactions [1]. The ^6Li reaction is most probable with a slow neutron; it is exothermic, releasing 4.8 MeV of energy. The ^7Li reaction is an endothermic reaction, only occurring with a fast neutron and absorbing 2.5 MeV of energy. Natural lithium is composed 92.6% of ^7Li and 6.4% of ^6Li thus an enrichment of the chosen breeder material is required. Considering that ^7Li reaction works with the high energy neutrons coming from the plasma, the decelerated neutron can still make a tritium atom by the ^6Li reaction thus creating two tritium atoms with one neutron [2]. The understanding of the kinetic dynamics of creation and release rate of this ion is crucial in order to achieve a reactor self-sustainable operation (Tritium Breeder Ratio, TBR higher than 1.15) [3] and can be strongly affected by the grain size, the porosity, the crystal structure and the degradation of the surface [4–6]. On the other hand the behaviour of lithium ions and its mobility are of special interest considering its central role inside the breeder material.

Lithium-containing ceramics, selected as the solid breeder for HCPB (Helium Cooled Pebble Bed) module, possess a series of advantages over liquid lithium and lithium–lead alloys. They have a sufficient lithium atom density (up to 540 kg $* m^{-3}$), high thermostability (up to 1300 K), chemical inertness [7], do not create ecological danger in the case of blanket dehermetization and have a good compatibility with structural materials [8]. Furthermore, being a non-mobile breeder, the selection of coolant that avoids problems related to safety or Magneto Hydro Dynamics (MHD) is possible, and the corrosion is limited only to punctual contacts with the structure of the blanket. The optimal design selected for these ceramics is the rounded one (with a diameter adjusted from 0.2 to 2.0 mm) in order to obtain a high packing density, a good thermal conductivity control, an improved mechanical stability and the capability of facilitating the flow of the purge gas [9], responsible for the transport of tritium out of the module. As a consequence the Spray-dryer technique has been identified as the best EU-process for the fabrication of Li_4SiO_4 spherical ceramics [10], though other methods are used and developed [11].

The electrical properties, an interesting tool for monitoring the microstructural changes of the ceramic material, are determined by the ionic movement in these ceramic materials. Considering that ionic conductivity in those insulators mostly occur if defects are present, it represents a method for monitoring the effect of the radiation-induced defects and of the impurities introduced in breeder blanket ceramics by the manufacturing process. The

* Corresponding author at: National Fusion Laboratory — CIEMAT, Avda. Complutense 40, 28040 Madrid, Spain. Tel.: +34 914962579; fax: +34 913466068.
E-mail address: elisabettacarella@gmail.com, elisabetta.carella@externos.ciemat.es (E. Carella).

http://dx.doi.org/10.1016/j.nme.2015.02.001

impedance spectroscopy (EIS) is thus employed to deconvolute the intrinsic or extrinsic contribution to the electrical properties by measuring the impedance response over a frequency spectrum (from 40 to 10^6 Hz) in as prepared and $5 * 10^5$ Gy irradiated pebbles [12,13].

2. Experimental procedure

2.1. Sample preparation and characterization

Lithium orthosilicate was prepared by Spray-dryer method. The dispersion was achieved with a pressure nozzle of 2 mm diameter (Mini Spray-dryer Buchi B-290), followed by pyrolysis at 200 °C in air using 0.4 Mol of silicon tetra-acetate and lithium acetate as starting solutions, dissolved in deionized water. The material was sprayed in co-current flow method. The spherical particles obtained were calcined at 800 °C during 2 h in air, in order to obtain a better crystallization.

Inductively Coupled Plasma (ICP) chemical analysis is a powerful tool for detecting and analysing trace and ultra-trace elements and it has been used to establish the nature of the impurities in the pebbles. The mass spectrometry was made using a High Resolution ELEMENT-XR (Thermo Fisher Scientific).

Crystallographic phases were monitored via X-ray diffraction (XRD-Philips diffractometer X-Pert-MPD) with a CuK_α-radiation source and a Si monochromator. The measurements were performed in Bragg–Brantano geometry [14]. The morphology of calcined particles and the microstructure of the sintered ceramics were observed by scanning electron microscopy (SEM-Hitachi S-2500) at 25 kV.

The samples were damaged by γ-irradiation through a ^{60}Co source (Nayade facility pool at CIEMAT-Madrid, Spain), at a fluence of 4.8 Gy/s at 50 °C to a total dose of $5 * 10^5$ Gy. After irradiation, the samples were characterized by impedance spectroscopy during heating treatments.

2.2. EIS (Electrochemical Impedance Spectroscopy)

The measurement of electrical resistivity versus thermal annealing treatments is one of the most widely used techniques to study the ionic defects and their transport properties in insulator materials [15]. When mobile charges are present, several physical processes may influence the data: bulk resistive–capacitive effects, bulk generation-recombination effects, electrode/interphase reactions, and diffusion along the grain.

Electrical Impedance Spectroscopy (EIS) is based on the measurements of electrical impedance (Z) over a frequency range (f) to obtain the impedance spectra. Experimental data may be approximated to the impedance of an equivalent circuit where the resistances are representative of bulk conductivity and capacitances are associated to the space charge polarization region. The EIS spectra were fitted using the "EQUIVCRT" (Equivalent Circuit Programme [16]). When Z imaginary and real components of Z were plotted in the Nyquist diagram, semicircles or semi-arcs were typically obtained.

Therefore, starting from the surface area (A), the thickness (e) and the resistance value (R) of the measured sample, the electrical conductivity was calculated as:

$$\sigma(T) = \frac{e}{A \circ R}. \quad (1)$$

According to the Arrhenius equation the relation between ionic conductivity in solids and the temperature T is given by:

$$\ln(\sigma T) = \ln \sigma_0 - \frac{E_A}{kT} \quad (2)$$

where E_A is the activation energy for the electrical conduction processes [12].

This technique is usually used to measure dense bodies; however it is possible to measure powdered samples if the holder is modified. This option is especially interesting in the case of the ceramic breeders made of pebbles for providing more realistic results in relation with the breeder blanket module situation.

In this work, a probe with two Pt-electrodes was used for EIS measurements, following the procedure described by Thomas [17]. The measurements were performed as a function of the temperature (RT-800 °C), in air and in the frequency range between 40 Hz and 10^6 Hz (Agilent 4294A). The pebbles were compacted in a Pt container (Fig. 1) which also acted as an electrode. The counter electrode (Pt slab) was located on the smooth surface of the compacted material.

3. Results

It is well known that the purity in phase and the microstructural characteristics of ceramics are significantly affected both, by the way of synthesis and by the temperature of sintering. Fig. 2 represents XRD diffraction patterns obtained after sintering, where the presence of the metasilicate (MSi, Li_2SiO_3) as secondary phase can be observed.

Table 1 shows the level of the impurities in the pebbles obtained by chemical analysis (ICP). The impurities identified are probably from the raw materials, considering that the used lithium-base from Sigma-Aldrich presents a purity of the 99.95% based on trace metal analysis.

The Fig. 3 shows the morphology of the "as prepared" powders fabricated by spray-dryer as observed by SEM images. A satisfactory spherical shape is achieved with an average size of 1 μm. Even if the

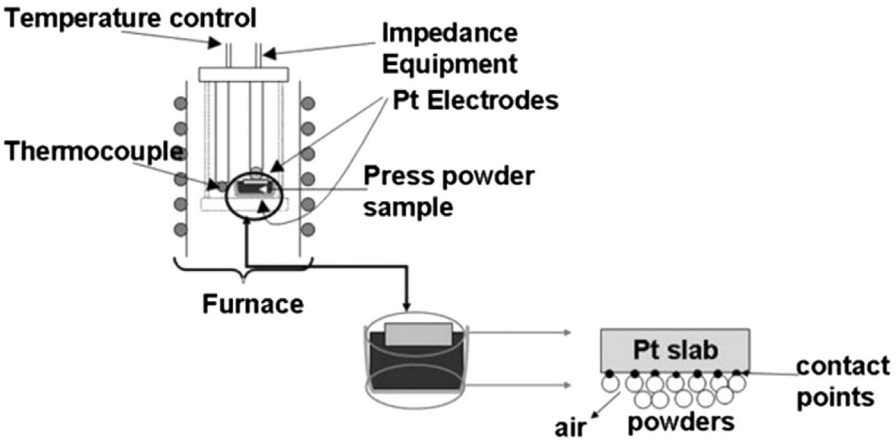

Fig. 1. Experimental scheme for the EIS measurements on Li_4SiO_4 pebbles in ICV laboratories. In the magnification, the sample holder designed for measurements of powder samples.

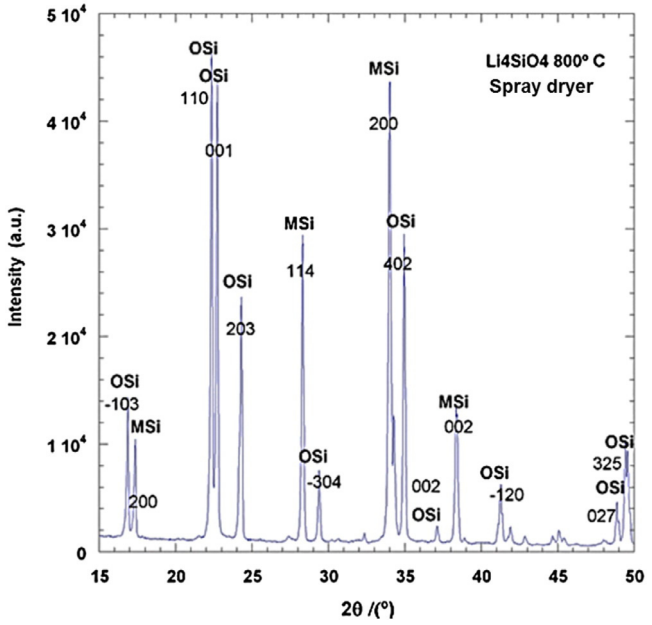

Fig. 2. XRD pattern of the pebble shaped ceramic powders obtained by Spray-dryer route, calcinated to a temperature of 800 °C/2 h. The peaks of two phases (OSi, orthosilicate and MSi, metasilicate) can be distinguished through Miller indices, indicating the atomic planes.

pebbles obtained are too small for fusion application, it is possible to improve their diameter by using a bigger nozzle [18].

The frequency-dependence of the resistance at different temperatures for the as prepared and irradiated pebbles at 500 kGy is shown in Figs. 4 and 5 respectively.

The behaviour of the samples shows the typical trend of a ceramic material, whose modulus of impedance decreases with temperature. Irradiation of the samples increases its resistance, fact that is more evident at higher temperatures (200–800 °C) where a difference of one order of magnitude can be appreciated. The variation with ionizing radiation found here can be due to the release of trapped charges and a consequent redistribution of the electrical configuration.

Nyquist plot of the imaginary vs. real part of Z, is presented here as an example to check the suitability of the proposed equivalent circuit. It shows two semicircle arcs (see Fig. 6), corresponding to different contributions to the charge carrier movement.

The first one at high temperatures is ascribed to the material itself bulk resistance; the second represents the charge transfer effect at the interphase material/electrodes. The second component appears with a high resistance value, because of the presence of air gaps. Once obtained the R values, it is possible to calculate the bulk conductivity as before mentioned.

The log of total electrical conductivity obtained from EIS spectra as a function of the inverse of temperature, is graphed in Fig. 7, evidencing that electrical conductivity is a thermally activated process and follows an Arrhenius trend.

The conductivity dependence on the temperature, also measured in previous work in the same temperature range [19], shows an extrinsic behaviour. The electrical conduction observed for the as-prepared material can be mainly caused by an ionic contribution. Its value before and after a low irradiation doses, presents a decrease of an order of magnitude at low temperature.

Table 1
Chemical analysis of the pebbles fabricated via spray-drying method.

Element	Al	Ca	Ce	Fe	Ti	Zr
Ppms (at)	1250	717	14	175	25	45

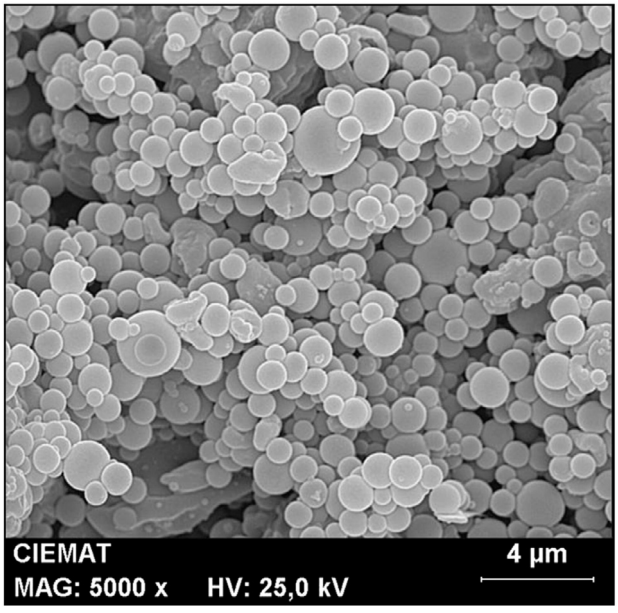

Fig. 3. SEM microstructure images of the as prepared Li_4SiO_4 ceramics fabricated by Spray-dryer method.

These results are emphasized in Table 2 where a comparison of the activation energy values calculated in three temperature ranges and of the conductivity at 400 °C is presented.

The temperature ranges selected are (1) between 800 and 700 °C, (2) between 650 and 500 °C and (3) between 400 and 200 °C. As expected, the energy necessary for activating the electrical conduction at low temperature is higher. The energy necessary for the activation of the electrical conduction always increases when the pebbles are irradiated. This confirms the hypothesis of a redistribution of the electrical configuration after gamma irradiation. Finally the same increase trend for the activation energy with temperature is observed in the damaged and undamaged case, confirming that the charge carriers responsible of the electrical conduction are not changed.

Finally it should be noted that the conductivity value of the Li_4SiO_4 fabricated in our laboratory at room conditions ($\sigma_{100\,°C} = 7.76 * 10^{-8}$ S/cm), is comparable to others found in literature ($\sigma_{100\,°C} \approx 10^{-8}$ S/cm) [20].

4. Discussion

Li_4SiO_4 is an ionic compound with a tetrahedral anion $(SiO_4)^{-4}$ structure [12] where silicon-ion is co-ordinated by 4 oxygen, and

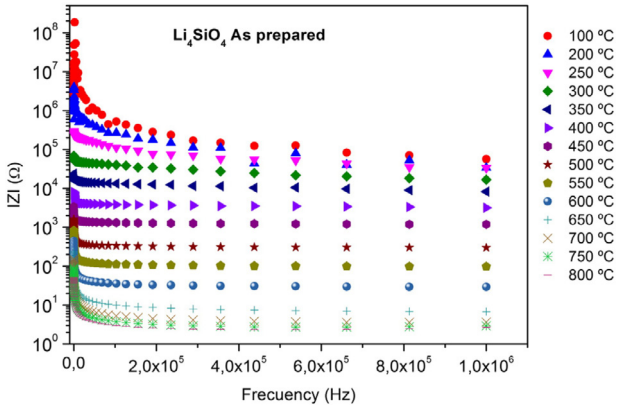

Fig. 4. Bode plot of the resistance vs. frequency for the Li_4SiO_4 pebbles before irradiation at the different temperatures explored during EIS analysis.

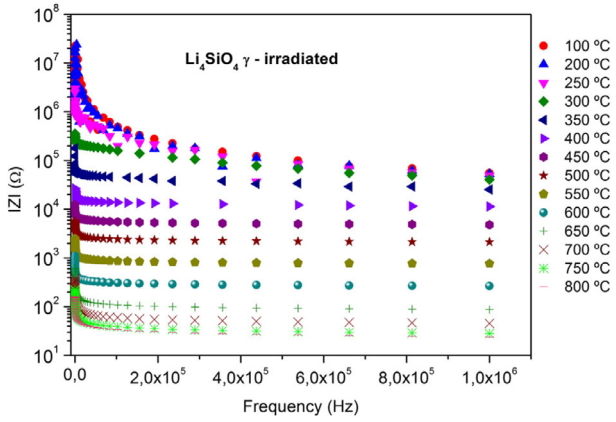

Fig. 5. Bode plot for the Li_4SiO_4 pebbles after irradiating to $5 * 10^5$ Gy total doses at different temperatures (from 100 to 800 °C).

lithium ions are floating around them in separate planes forming the so called "cation channels". The positional parameters of Li, Si and O atoms are referred to those given by Baur [21]. In this structure there is one type of Si atoms, three types of O atoms and 6 types of Li atoms. Considering the crystal lattice structure and following ab-initio suggestions [22] the conducting species are presumed to be Li^+ although O ions may be mobile to a certain extent. The creation of defects acting as traps [23] and the introduction of impurities during fabrication process, should alter the electronic band gap, resulting in a modification of the electrical conductivity [24].

The calculated band gap of 5.53 eV [25] at room temperature reveals the non-conductive nature of lithium orthosilicate. The insulator behaviour of these ceramics makes them sensitive to ionization damage with the result that electrical properties may be modified also for low irradiation total doses. The ionic components as charge carriers (like Li^+) are the causing agent for the electrical conduction observed in the as prepared samples. At the same time, the presence of impurities (see Table 1) could affect the charge movement, facilitating it. The reduction in conductivity observed in the damaged samples can be explained as a recombination of the free charge carriers thanks to the electrical excitation due to γ-radiation which causes a decrease in the total electrical conduction [26]. As observed by the authors in previous works [27], the reorganization of the electrical configuration of these insulating materials can cause a decrease or an increase of the total conductivity in the volume, depending on the change caused by the radiation-dose and the movement of the

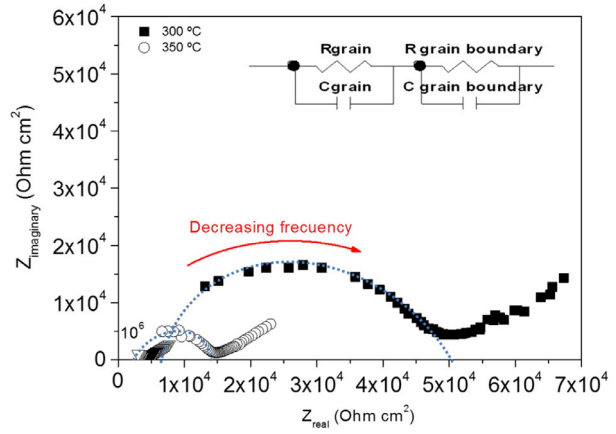

Fig. 6. Nyquist plot of the Li_4SiO_4 pebbles after a γ-ray doses of $5 * 10^6$ Gy measured in the temperature range between 500 and 650 °C. In the inset the plots obtained from 300 to 400 °C.

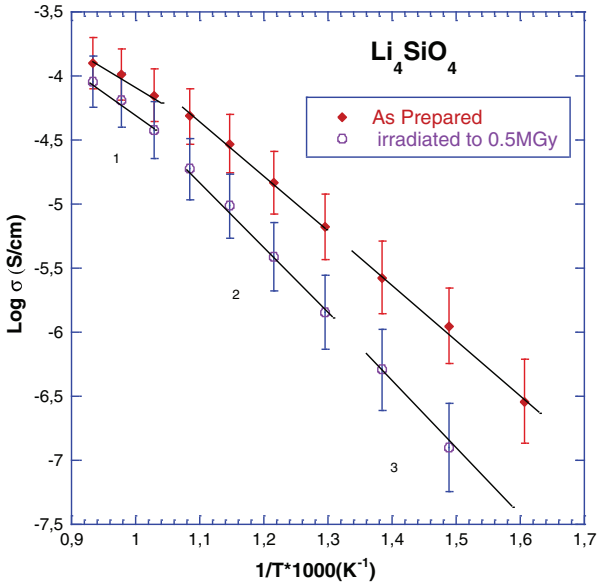

Fig. 7. Total conductivity for the Li_4SiO_4 pebbles in the case of as-prepared (red circle) and irradiated (green star) ceramics represented in an Arrhenius plot. The slope of the curve is proportional to the activation energy for the electrical processes occurring in the materials. Three processes can be identified.

charge carriers. At the same time it is important to consider the role played by impurities in the stability of this breeder blanket candidate. Considering that impurities will be always present during the fabrication process and that reprocessing could increase their percentage [28,29], it is important to observe the physic-chemical stability of this material with time.

In relation with the temperature dependence, a slight decrease of the activation energy at increasing temperatures has been observed, in both undamaged and damaged case. The increasing ratio is quite the same, indicating that the same process is occurring in both cases under thermal excitation: the charge carriers, mostly ions, are able to move easily inside the crystal structure.

It has been demonstrated that EIS measurements show similar electrical responses and the same electrical conduction mechanism in the case of as prepared and low-damaged cases. Considering the importance of the physic-chemical stability of this insulator ceramic inside the breeder blanket structure, the electrical stability found is desirable. Finally it is possible to speculate that considering the bigger diameter of the official BB candidate pebbles, a lower contact surface among them will ensure a lower electrical conduction.

5. Conclusions

The electrical behaviour of the undamaged ceramic and the activation energy values calculated reveals a crystal structure in which Li^+ ions are identified as the conducting species. The damage introduced by a dose of $5 * 10^{15}$ Gy of gamma irradiation creates a soft reduction of the electrical conduction process, quite totally recovered by the annealing treatments up to 800 °C.

Table 2
Conductivity value at 400 °C and activation energy in three temperature ranges calculated for the Li_4SiO_4 damaged and undamaged ceramic.

Li_4SiO_4	As prepared	Irradiated at $5 * 10^5$ Gy
1° E_A (eV)	0.78 ± 0.03	1.03 ± 0.05
2° E_A (eV)	0.81 ± 0.04	1.05 ± 0.05
3° E_A (eV)	0.87 ± 0.04	1.09 ± 0.05
σ(S/cm)	$1.12 * 10^{-6}$	$1.25 * 10^{-7}$

Li_4SiO_4 ceramic, selected as the EU candidate for ITER testing does not present any drastic change in its electrical properties, confirming its stability and durability.

The exposure of Li_4SiO_4 pebble powders to γ-radiation has provided information on the electrical properties, thus revealing the possibility of employing electrical measurements for controlling the properties of ceramic materials for specific technological applications.

Acknowledgements

The authors are indebted to Mrs Montserrat Martín and David Bravo for their help in these experiments. This work has been supported by the Spanish Ministry of Economic and Competitiveness under Radiafus III project ENE2012-39787-C06-0. Dra. Moreno acknowledged the FSE for the financial support of her JAE-Doc contract.

References

[1] G. McCracken, P. Stott, Fusion: the Energy of the Universe, Academic Press, 2012.
[2] D. Clery, A Piece of the Sun: the Quest for Fusion Energy, 2013.
[3] M.E. Sawan, M.A. Abdou, Fusion Eng. Des. 81 (2006) 1131–1144, doi:10.1016/j.fusengdes.2005.07.035.
[4] L. Padilla-Campos, J. Mol. Struct. THEOCHEM 621 (2003) 107–112, doi:10.1016/s0166-1280(02)00538-9.
[5] A. Vitins, G. Kizane, J. Tiliks, J. Tiliksjr, E. Kolodinska, Fusion Eng. Des. 82 (2007) 2341–2346, doi:10.1016/j.fusengdes.2007.06.011.
[6] H. Ohno, J. Nucl. Mater. 133–134 (1985) 181–185, doi:10.1016/0022-3115(85)90130-8.
[7] A.R. Raffray, M. Akiba, V. Chuyanov, L. Giancarli, S. Malang, J. Nucl. Mater. 307–311 (2002) 21–30, doi:10.1016/s0022-3115(02)01174-1.
[8] J.E. Tiliks, G.K. Kizane, A.A. Supe, A.A. Abramenkovs, J.J. Tiliks, V.G. Vasiljev, Fusion Eng. Des. 17 (1991) 17–20, doi:10.1016/0920-3796(91)90029-p.
[9] Z. An, A. Ying, M. Abdou, Fusion Eng. Des. 82 (2007) 2233–2238, doi:10.1016/j.fusengdes.2007.02.004.
[10] R. Knitter, B. Alm, G. Roth, J. Nucl. Mater. 367–370 (Part B) (2007) 1387–1392, doi:10.1016/j.jnucmat.2007.04.002.
[11] J. Lulewicz, J. Nucl. Mater. 307–311 (2002) 803–806, doi:10.1016/s0022-3115(02)00981-9.
[12] A.R. West, J. Appl. Electrochem. 3 (1973) 327–335, doi:10.1007/bf00613041.
[13] J.R. Macdonald, Ann. Biomed. Eng. 20 (1992) 289–305, doi:10.1007/BF02368532.
[14] L.A. Aslanov, G.V. Fetisov, J.A.K. Howard, Crystallographic Instrumentation, International Union of Crystallography; Oxford University Press, [Chester, England]; Oxford; New York, 1998.
[15] S. Konishi, H. Ohno, J. Am. Ceram. Soc. 67 (1984) 418–419, doi:10.1111/j.1151-2916.1984.tb19727.x.
[16] Bernard A. Boukamp, EQUIVCRT Software, University of Twente, Enschede, Netherlands, 1993.
[17] G. Thomas, Solid State Ion. 101–103 (1997) 775–780, doi:10.1016/s0167-2738(97)00293-2.
[18] R. Knitter, M. Kolb, U. Kaufmann, A. Goraieb, J. Nucl. Mater. 442 (2013) S433–S436, doi:10.1016/j.jnucmat.2012.10.034.
[19] E. Carella, T. Hernández, Phys. B Condens. Matter 407 (2012) 4431–4435, doi:10.1016/j.physb.2012.07.013.
[20] C.-H. Doh, A. Veluchamy, M.-W. Oh, B.-C. Han, J. Electrochem. Sci. Technol. 2 (2011) 146–151, doi:10.5229/JECST.2011.2.3.146.
[21] W.H. Baur, T. Ohta, J. Solid State Chem. 44 (1982) 50–59, doi:10.1016/0022-4596(82)90400-5.
[22] K. Munakata, Y. Yokoyama, J. Nucl. Sci. Technol. 38 (2001) 915–918, doi:10.1080/18811248.2001.9715117.
[23] A. Abramenkovs, J. Tiliks, G. Kizane, V. Grishmanovs, J. Nucl. Mater. 248 (1997) 116–120, doi:10.1016/s0022-3115(97)00206-7.
[24] X. Li, H. Guo, L. Li, X. Li, Z. Wang, H. Ou, et al., Trans. Nonferrous Met. Soc. China 21 (2011) 529–534, doi:10.1016/s1003-6326(11)60747-4.
[25] T. Tang, P. Chen, W. Luo, D. Luo, Y. Wang, J. Nucl. Mater. 420 (2012) 31–38, doi:10.1016/j.jnucmat.2011.08.040.
[26] M. Nagai, M. Hibino, T. Nishino, K. Noda, J. Mater. Sci. Lett. 12 (1993) 107–109, doi:10.1007/bf00241862.
[27] E. Carella, T. Hernández, Fusion Eng. Des. 90 (2015) 73–78, doi:10.1016/j.fusengdes.2014.11.010.
[28] R. Knitter, U. Fischer, S. Herber, C. Adelhelm, J. Nucl. Mater. 386–388 (2009) 1071–1073, doi:10.1016/j.jnucmat.2008.12.284.
[29] R. Knitter, B. Lobbecke, J. Nucl. Mater. 361 (2007) 104–111, doi:10.1016/j.jnucmat.2006.11.005.